Journal of the American College of Cardiology
© 2014 by the American College of Cardiology Foundation
Published by Elsevier Inc.

Vol. 63, No. 8, 2014
ISSN 0735-1097/$36.00
http://dx.doi.org/10.1016/j.jacc.2013.07.119

Cardiac Imaging

Multiparametric Cardiovascular Magnetic Resonance Assessment of Cardiac Allograft Vasculopathy

Christopher A. Miller, BSc, MBChB,*†‡ Jaydeep Sarma, MA, MB BChir, PhD,*‡ Josephine H. Naish, PhD,† Nizar Yonan, MD,*‡ Simon G. Williams, MD,*‡ Steven M. Shaw, PhD,*‡ David Clark, BSc,§ Keith Pearce, BSc,* Martin Stout, PhD,* Rahul Potluri, MBChB,*† Alex Borg, MD,* Glyn Coutts, PhD,|| Saqib Chowdhary, PhD,*‡ Gerry P. McCann, MD,¶ Geoffrey J. M. Parker, PhD,† Simon G. Ray, MD,*‡ Matthias Schmitt, MD, PhD*‡

Manchester and Leicester, United Kingdom

Objectives This study sought to evaluate the diagnostic performance of multiparametric cardiovascular magnetic resonance (CMR) for detecting cardiac allograft vasculopathy (CAV) using contemporary invasive epicardial artery and microvascular assessment techniques as reference standards, and to compare the performance of CMR with that of angiography.

Background CAV continues to limit the long-term survival of heart transplant recipients. Coronary angiography has a Class I recommendation for CAV surveillance and annual or biannual surveillance angiography is performed routinely in most centers.

Methods All transplant recipients referred for surveillance angiography at a single UK center over a 2-year period were prospectively screened for study eligibility. Patients prospectively underwent coronary angiography followed by coronary intravascular ultrasound, fractional flow reserve, and index of microcirculatory resistance. Within 1 month, patients underwent multiparametric CMR, including assessment of regional and global ventricular function, absolute myocardial blood flow quantification, and myocardial tissue characterization. In addition, 10 healthy volunteers underwent CMR.

Results Forty-eight patients were recruited, median 7.1 years (interquartile range: 4.6 to 10.3 years) since transplantation. The CMR myocardial perfusion reserve was the only independent predictor of both epicardial ($\beta = -0.57$, $p < 0.001$) and microvascular disease ($\beta = -0.60$, $p < 0.001$) on stepwise multivariable regression. The CMR myocardial perfusion reserve significantly outperformed angiography for detecting moderate CAV (area under the curve, 0.89 [95% confidence interval (CI): 0.79 to 1.00] vs. 0.59 [95% CI: 0.42 to 0.77], $p = 0.01$) and severe CAV (area under the curve, 0.88 [95% CI: 0.78 to 0.98] vs. 0.67 [95% CI: 0.52 to 0.82], $p = 0.05$).

Conclusions CAV, including epicardial and microvascular components, can be detected more accurately using noninvasive CMR-based absolute myocardial blood flow assessment than with invasive coronary angiography, the current clinical surveillance technique. (J Am Coll Cardiol 2014;63:799–808) © 2014 by the American College of Cardiology Foundation

Cardiac allograft vasculopathy (CAV) continues to represent the major limitation to long-term survival in heart transplant recipients (1). CAV is characterized by diffuse coronary intimal and medial thickening. It affects both the epicardial arteries and the microvessels; however, it does so independently, and epicardial and microvascular disease are both independently predictive of prognosis (2–4). Because of denervation of the transplanted heart, CAV usually does not

From the *North West Heart Centre and Transplant Centre, University Hospital of South Manchester, Wythenshawe Hospital, Manchester, United Kingdom; †Centre for Imaging Sciences and Biomedical Imaging Institute, University of Manchester, Manchester, United Kingdom; ‡Institute of Cardiovascular Sciences, University of Manchester, Manchester, United Kingdom; §Alliance Medical Cardiac MRI Unit, Wythenshawe Hospital, Manchester, United Kingdom; ||Christie Medical Physics and Engineering, Christie Hospital, Manchester, United Kingdom; and the ¶NIHR Leicester Cardiovascular Biomedical Research Unit and Department of Cardiovascular Sciences, University of Leicester, Leicester, United Kingdom. Dr. Miller is supported by a Fellowship from the National Institute for Health Research, United Kingdom (NIHR-DRF-2010-03-98). Drs. Miller, Yonan, Williams, and Schmitt have received research funding from the New Start Transplant Charity, United Kingdom. Dr. McCann is supported by a Fellowship from the National Institute for Health Research, United Kingdom (NIHR-PDF-2011-04-51). Dr. Parker is a director and shareholder of Bioxydyn, Ltd. All the other authors have reported they have no relationships relevant to the contents of this paper to disclose.

Manuscript received April 2, 2013; revised manuscript received June 21, 2013, accepted July 15, 2013.

Abbreviations and Acronyms

CAV = cardiac allograft vasculopathy

CMR = cardiovascular magnetic resonance

FFR = fractional flow reserve

IMR = index of microcirculatory resistance

IVUS = intravascular ultrasonography

LAD = left anterior descending coronary artery

LGE = late gadolinium enhancement

MBF = myocardial blood flow

MPR = myocardial perfusion reserve

ROC = receiver-operating characteristic

ROI = region of interest

become clinically apparent until it has progressed to an advanced stage, when sequelae such as myocardial infarction, progressive heart failure, or arrhythmic sudden death ensue. Screening is therefore required for its early detection.

Coronary intravascular ultrasonography (IVUS) is considered the gold standard technique for diagnosing CAV; however, its broad clinical use in this context is limited by cost and lack of widespread expertise, and its evaluation is limited to epicardial vessels (5). Invasive coronary angiography has a low sensitivity for detecting CAV because of the diffuse nature of the disease with a lack of normal reference segments, and relatively late occurring luminal narrowing (6). Furthermore, angiography is associated with significant, albeit uncommon, complications, and repeated studies are costly and carry a considerable cumulative radiation burden. However, despite these shortcomings, angiography has a Class I recommendation for CAV screening, and annual or biannual surveillance angiography is performed routinely in most centers (7).

Noninvasive imaging approaches to the detection of CAV offer a number of theoretical advantages; however, the findings of the majority of studies assessing their diagnostic performance have been unconvincing (8). Importantly, most such studies have been limited by the use of coronary angiography as the reference standard, with stenoses of 50% or 70% as the significance thresholds, despite adverse events frequently occurring well before such advanced disease is reached (9). Furthermore, none has included reference assessment of the microvasculature.

Cardiovascular magnetic resonance (CMR) is a potentially attractive screening modality for CAV due to its lack of ionizing radiation and its multiparametric nature, namely, its ability to assess multiple aspects of pathology in a single examination (including ventricular function, myocardial perfusion, and myocardial tissue characterization). Systematic evaluation of multiparametric CMR for the diagnosis of CAV has not been reported to date. The aim of this study was to evaluate the diagnostic performance of multiparametric CMR in CAV, and to compare it with that of invasive coronary angiography, using contemporary invasive epicardial artery and microvascular assessment techniques as reference standards.

Methods

Patients and study design. All heart transplant recipients referred for CAV surveillance coronary angiography at University Hospital of South Manchester NHS Trust, United Kingdom (1 of 6 UK adult heart transplant centers), between November 1, 2010, and November 1, 2012, were prospectively screened for study eligibility (Fig. 1). Patients were excluded if they had a contraindication to CMR or adenosine infusion, an estimated glomerular filtration rate of 35 ml/min/1.73 m^2 or less, or current confirmed or suspected acute allograft rejection.

In addition, 10 age- and sex-matched healthy volunteers were recruited. The volunteers were completely asymptomatic with no known risk factors or history of cardiac disease, normal physical examination, and normal electrocardiogram (i.e., they were not patients who had been referred for CMR that was subsequently found to be normal).

Patients underwent coronary angiography, followed immediately by invasive coronary physiological measurements and coronary intravascular ultrasonography (IVUS) as described in the following text. Within 1 month of the invasive investigations, patients underwent multiparametric CMR assessment. The order of the invasive assessment and CMR was determined randomly, and no patient had an interim cardiovascular event. Healthy volunteers underwent CMR only. An ethics committee of the UK National Research Ethics Service approved the study, and written informed consent was obtained from all participants. The work was conducted according to the Helsinki Declaration.

Invasive investigations. CORONARY ANGIOGRAPHY. Coronary angiography was performed according to the standard Judkin technique with a 6F system. Multiple projections of the coronary arteries were acquired, including at least 2 orthogonal views of the proximal, mid, and distal left anterior descending (LAD) artery.

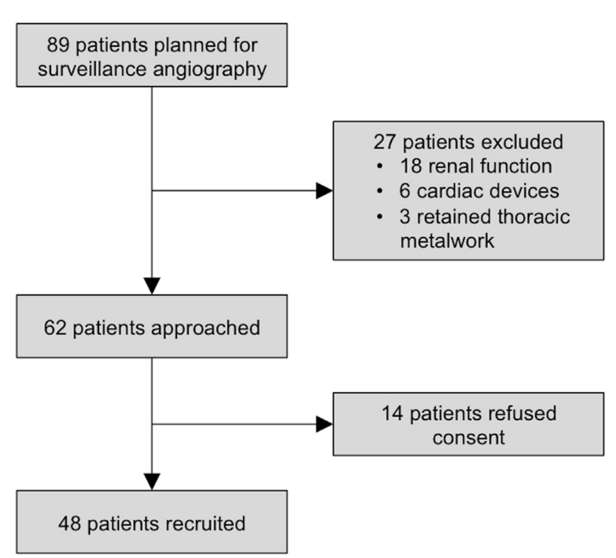

Figure 1 **Recruitment Data**

The number of patients approached, excluded, and recruited.

PHYSIOLOGICAL MEASUREMENTS. After acquiring the angiographic images, 70 IU/kg heparin was administered intravenously, and a 6-F guiding catheter was used to engage the left coronary artery. Intracoronary nitroglycerin (200 μg) was given. A 0.014-inch coronary pressure wire (Radi Medical Systems, St. Jude Medical, St. Paul, Minnesota) was calibrated, equalized, and advanced to the distal portion of the LAD. Maximal hyperemia was induced by administration of intravenous adenosine (140 μg/kg/min) through a 18G cannula in a large peripheral vein for 3 min before and during data acquisition. Hyperemic mean transit time was determined by averaging the transit times of 3 × 3 ml boluses of room temperature saline. Mean aortic and distal coronary pressures were recorded. Meticulous attention was paid to guide catheter engagement. Fractional flow reserve (FFR) was calculated by dividing the mean distal coronary pressure by the mean proximal coronary pressure during hyperemia. Index of microcirculatory resistance (IMR) was calculated by multiplying the distal coronary pressure by the hyperemic mean transit time, measured simultaneously (10).

INTRAVASCULAR ULTRASONOGRAPHY. After the physiological measurements, a 40 MHz IVUS catheter (Atlantis SR Pro, Boston Scientific, Natick, Massachusetts) was advanced over the wire, so that the transducer was positioned in the distal artery, as close as possible to the pressure transducer mounted on the pressure wire. Automated pullback at a constant rate of 0.5 mm/s was performed along the length of the vessel.

Cardiovascular magnetic resonance. The CMR was performed using a 1.5-T scanner (Avanto, Siemens Medical Imaging, Erlangen, Germany) equipped with a 32-element phased-array coil.

GLOBAL AND REGIONAL LEFT VENTRICULAR FUNCTION. Steady-state free precession cine images were acquired in standard long-axis views and in a stack of short-axis slices covering the left ventricle (LV). Short-axis tagged images were acquired at basal, mid, and apical ventricular levels using a segmented k-space fast gradient echo sequence with spatial modulation of magnetization in orthogonal planes.

PERFUSION. Using a saturation recovery gradient echo sequence, basal, mid, and apical short-axis images were acquired every heartbeat during pharmacological vasodilation (“stress”) and at rest. For stress imaging, intravenous adenosine (140 μg/kg/min) was administered through a 18G cannula in a large peripheral vein for 3 min before, and during, data acquisition. A 0.05 mmol/kg bolus of gadolinium-based contrast agent (gadopentetate dimeglumine [Gd-DTPA]; Magnevist, Bayer HealthCare, Wuppertal, Germany) was administered intravenously at 5 ml/s followed by a 30-ml saline flush. Rest imaging was performed 10 min after stress imaging with a further 0.05 mmol/kg of contrast agent. After rest perfusion image acquisition, a further 0.1 mmol/kg of contrast agent was administered to bring the total dose to 0.2 mmol/kg.

TISSUE CHARACTERIZATION. A single-shot modified Look Locker inversion recovery sequence was acquired in short-axis view at midventricular level before the contrast agent was administered, and 15 min after the final dose of the contrast agent (11). Blood samples were taken at the time of CMR to measure hematocrit. Standard late gadolinium enhancement imaging was performed at least 10 min after the final dose of the contrast agent using spoiled gradient echo segmented inversion recovery and phase-sensitive inversion recovery segmented gradient echo sequences.

Image analysis. QUANTITATIVE CORONARY ANGIOGRAPHY. Angiographic images were analyzed using quantitative coronary angiography, performed on the proximal, mid, and distal LAD with guiding catheter calibration (QAngio XA, Medis Medical Imaging Systems, Leiden, the Netherlands). Reference and minimal lumen diameters for the 3 sites were measured, and the greatest percent diameter stenosis was recorded.

INTRAVASCULAR ULTRASOUND. Quantitative analysis was performed using QIVUS (Medis Medical Imaging Systems), according to the method described by Fearon et al. (12). The external elastic lamina and luminal border were traced on images acquired every 0.1 mm. “Plaque area” (also known as intima-media area) was calculated as vessel area minus luminal area. By means of Simpson’s method, vessel volume, luminal volume, and hence, plaque volume were calculated as the sum of the respective areas multiplied by the “segment” length of 0.1 mm. Subsequently the plaque volume index, defined as plaque volume expressed as a percentage of vessel volume, was calculated to normalize for vessel size and length of IVUS pullback.

Cardiovascular magnetic resonance. FUNCTIONAL ANALYSIS. The LV mass, end-diastolic volume, end-systolic volume, and ejection fraction (EF) were quantified from steady-state free precession images using CMRtools (Cardiovascular Imaging Solutions, London, United Kingdom) (13). Peak systolic circumferential strain (εcc) and strain rate (systolic and early diastolic) were measured from midventricular short-axis tagged images using SinMod (inTag software, version 5.0, CREATIS Laboratory, Lyon, France; and Maastricht University, the Netherlands) (14). Basal and apical short-axis rotation, calculated from basal and apical tagged images using the same software, and epicardial areas, measured on corresponding steady-state free precession images, were incorporated into a custom-written algorithm (Microsoft Excel using Visual Basic). After expression of time coordinates as a percentage of systolic duration (time between peak electrocardiogram R-wave and aortic valve closure) and cubic spline interpolation, twist was calculated by subtracting basal rotation from apical rotation at each time point. Normalized twist was calculated as the twist angle divided by distance between basal and apical slice positions. Torsion (represented by an approximation of the circumferential-longitudinal shear angle) was calculated by multiplying normalized twist by the mean of the basal and apical epicardial radii at each time point.

PERFUSION QUANTIFICATION. Endocardial and epicardial contours were drawn on the perfusion images using Osirix Imaging Software, version 4.0 (Pixmeo, Geneva, Switzerland). An additional region of interest (ROI) was drawn in the blood pool on the basal images, avoiding papillary muscles and trabeculae. The ROIs were manually translated on each perfusion image of the same slice to compensate for rigid-body translational motion. Perfusion quantification was performed in MatLab, version R2009a (MathWorks, Natick, Massachusetts) using algorithms written in house. Signal intensity curves were extracted from the average signal in the blood pool, to provide an arterial input function, and on a voxel-wise basis from the myocardial ROI. Signal intensity was converted to contrast agent concentration (15). Data for quantitative perfusion analysis were restricted to the first pass of the contrast agent through the heart, which was automatically detected from the blood pool signal curve. Perfusion values were obtained on a voxel-wise basis using generalized Tikhonov deconvolution with a b-spline representation of the impulse response function (16). Myocardial perfusion reserve (MPR) was calculated by dividing median hyperemic myocardial blood flow (MBF) by median resting MBF.

TISSUE CHARACTERIZATION. The LGE images were reported visually by 2 experienced operators, and the presence or absence of LGE, and its distribution pattern, were recorded. Myocardial T1 relaxation time was measured by drawing endocardial and epicardial contours on the modified Look Locker inversion recovery images using Osirix Imaging Software, version 4.0 (Pixmeo). In keeping with Wong et al. (17), myocardium in the vicinity of infarcted myocardium was excluded, but foci of LGE in myocardium free from infarction were not excluded. An additional ROI was drawn in the blood pool for measurement of blood T1. The ROIs were manually translated on each effective inversion time (TIeff) image to compensate for rigid-body translational motion. To obtain voxel-wise T_1 relaxation maps, a 3-parameter fit to the signal intensity, S as a function of TIeff was performed according to $S(TIeff) = A - Be^{(-TIeff/T1^*)}$, and T_1 was calculated as $T_1 = T_1^*((B/A) - 1)$. Fitting was carried out using MatLab, version R2009a (MathWorks). After applying a heart-rate correction algorithm, mean midventricular pixel T_1 relaxation times before and after contrast were then used to calculate myocardial extracellular volume according to the following formula: extracellular volume fraction (ECV) $= \lambda \times (1-$ hematocrit), where the partition coefficient, $\lambda = \Delta R_1(\text{myocardium}) / \Delta R_1(\text{blood})$. The ΔR_1 is proportional to contrast agent concentration: $\Delta R_1 = R_1(\text{post-contrast}) - R_1(\text{pre-contrast})$.

Statistical analysis. All data were analyzed in a blinded fashion, with independent analysis of CMR and invasive data. The IVUS plaque volume index and IMR were used as the reference standards for epicardial and microvascular disease, respectively (see the Discussion section). Statistical analysis was performed using SPSS, version 19 (IBM, Armonk, New York), and STATA, version 11.0 (StataCorp, College Station, Texas). Continuous variables are expressed as mean ± SD unless stated. An independent-samples *t* test (or Mann-Whitney *U* test where appropriate) was used to compare data from transplant patients and healthy volunteers. Linear regression was used to investigate possible associations between continuous invasive and CMR data, and stepwise selection methods were used to determine the most important associations. Separate stepwise analyses were performed for the angiographic and CMR data. Because of the relatively small size of the study, the number of univariable associations entered into the multivariable model was limited to 5, and overlapping variables were avoided. Receiver-operating characteristic (ROC) curve analyses were used to determine optimal cut-off points for CMR MPR and coronary angiographic stenosis, respectively, for detecting CAV (epicardial and microvascular disease), and estimates of sensitivity and specificity were derived. Given the absence of well-defined severity thresholds, the 75th centile ("severe disease") and median values ("moderate disease") for both plaque volume index and IMR were used to define the presence of epicardial and microvascular disease, respectively. The diagnostic performance of CMR MPR and coronary angiography were compared using a chi-square comparison of the trapezoidal area under the respective ROC curves.

Results

Study population. Forty-eight patients were recruited (Fig. 1). In 2 patients the LAD was occluded, meaning that IVUS and invasive coronary physiological assessment were not possible (for the purpose of the subsequent ROC curve analyses, both were considered to have severe epicardial

Table 1 Subject Characteristics

	Transplant Patients (n = 48)	Healthy Volunteers (n = 10)	p Value
Male	41 (85%)	8 (80%)	0.674
Age, yrs	51 ± 14	48 ± 8	0.560
Male	52 ± 13	48 ± 8	0.377
Female	46 ± 19	51 ± 10	0.742
Nonwhite	5 (10%)	1 (10%)	0.969
Weight, kg	86.0 ± 16.3	82.1 ± 12.5	0.471
Height, m	1.71 ± 0.06	1.77 ± 0.10	0.015
BSA, m^2	1.98 ± 0.19	1.99 ± 0.18	0.841
BMI, kg/m^2	29.4 ± 4.9	26.3 ± 4.0	0.066
eGFR, $ml/min/m^2$	58 ± 16	87 ± 13	<0.001
HR, beats/min	80 ± 12	61 ± 7	<0.001
Systolic BP, mm Hg	124 ± 18	114 ± 9	0.079
Diastolic BP, mm Hg	78 ± 12	69 ± 6	0.030
RPP	9.83 ± 1.75	6.92 ± 1.22	<0.001

Values are n (%) or mean ± SD.
BMI = body mass index; BP = blood pressure; BSA = body surface area; eGFR = estimated glomerular filtration rate; HR = heart rate; RPP = rate pressure product (systolic blood pressure × heart rate × 0.001).

disease). Three patients underwent CMR without gadolinium contrast (estimated glomerular filtration rate deteriorated to <35 ml/min/1.73 m^2 between the invasive studies and CMR in 2 patients, and 1 patient terminated the scan early because of claustrophobia). There were no complications. Demographic data are presented in Table 1 and Online Table 1. Median time from transplantation to enrollment was 7.1 years (interquartile range: 4.6 to 10.3 years).

Invasive investigations. Mean plaque volume index was 22.4 ± 9.8% and mean maximal intima-media thickness was 1.21 ± 0.57 mm. Mean FFR was 0.90 ± 0.06. An FFR <0.80 was observed in 1 patient (2%). Mean IMR was 23.7 ± 12.5. There was a significant correlation between plaque volume index and FFR (r = −0.46, p = 0.001), but there was no correlation between plaque volume index and IMR (r = 0.24, p = 0.103). The FFR was seen to improve as IMR deteriorated (r = 0.32, p = 0.028).

Mean maximum angiographic stenosis was 23.9 ± 16.0%. Maximum angiographic stenosis showed a significant correlation with plaque volume index (r = 0.33, p = 0.024) and FFR (r = −0.38, p = 0.010). There was no correlation between maximum angiographic stenosis and IMR (r = −0.16, p = 0.281).

Cardiovascular magnetic resonance. The CMR data are presented in Table 2 and Online Table 2. In keeping with the significantly higher resting rate pressure product seen in transplant patients (Table 1), resting MBF was significantly higher in transplant patients than in healthy volunteers. Stress MBF was significantly lower in transplant recipients compared with healthy volunteers, as was MPR. Significant differences were also seen between transplant patients and healthy volunteers in indexed LV end-diastolic volume, εcc, and twist, but not in normalized twist, torsion, or time to peak torsion (i.e., time to onset of untwisting). Atypical LGE was seen in almost half of transplant recipients, and 4 of those (9% of the study population) also had infarct-typical LGE. Inferior right ventricular septal insertion point enhancement was the most common type of atypical LGE (16 patients; 36%), but midwall (5 patients; 11%), "punched-out" (4 patients; 9%) and epicardial (2 patients; 4%) patterns were also observed. Pericardial LGE was observed in 3 patients (7%). Myocardial ECV was significantly higher in transplant patients compared with healthy volunteers.

Associations with plaque volume index. On univariable analysis, maximum angiographic stenosis showed a significant association with plaque volume index; however, after correcting for time since transplantation, this relationship was no longer significant (p = 0.295) (Table 3, Online Table 3). Early diastolic strain rate, stress MBF, MPR and infarct LGE were significantly associated with plaque volume index on univariable analyses, but only MPR and early diastolic strain rate remained independently associated with plaque volume index on multivariable analysis (Fig. 2A).

Associations with index of microcirculatory resistance. Maximum angiographic stenosis was not significantly associated with IMR on univariable analysis (Table 4). Patient

Table 2 Comparison of Cardiovascular Magnetic Resonance Findings in Transplant Patients and Healthy Volunteers

	Transplant Patients (n = 48)	Healthy Volunteers (n = 10)	p Value
LVEDVI, ml/m^2	74.5 ± 15.1	86.6 ± 7.7	0.018
LVESVI, ml/m^2	28.0 ± 8.8	28.2 ± 4.4	0.951
LV stroke volume index, ml/m^2	46.5 ± 9.5	58.4 ± 6.5	<0.001
LVEF, %	62.9 ± 7.6	67.5 ± 4.3	0.069
LVMI, g/m^2	50.0 ± 11.3	47.8 ± 7.3	0.544
εcc, %	−14.48 ± 3.33	−20.4 ± 1.48	<0.001
Twist, degree	9.08 ± 3.38	12.42 ± 3.45	0.007
Resting MBF, ml/min/g	0.86 ± 0.10	0.74 ± 0.09	0.001
Stress MBF, ml/min/g	1.50 ± 0.40	1.77 ± 0.24	0.043
MPR	1.74 ± 0.45	2.42 ± 0.36	<0.001
LGE (n = 45)	22 (49%)	0	
Infarct LGE	4 (9%)	0	
Atypical LGE	22 (49%)	0	
Myocardial ECV, %	29.0 ± 4.3	25.3 ± 1.8	0.011

Values are mean ± SD. The suffix "I" indicates indexed to body surface area. Additional data can be found in the Online Table 2.

ECV = extracellular volume; EDV = end-diastolic volume; EF = ejection fraction; εcc = peak systolic circumferential strain; ESV = end-systolic volume; LGE = late gadolinium enhancement; LV = left ventricle; MBF = myocardial blood flow; MPR = myocardial perfusion reserve; SV = stroke volume.

Table 3 Associations With Intravascular Ultrasound Plaque Volume Index

Univariable Associations	β	p Value
Patient characteristics		
Age	0.15	0.325
Time since transplantation	0.49	0.001
Donor age	0.29	0.058
Angiography		
Maximum angiographic stenosis	0.33	0.024
CMR		
LVEF	0.17	0.257
LVMI	0.18	0.229
εcc	0.17	0.263
Early diastolic SR	−0.38	0.014
Resting MBF	0.10	0.515
Stress MBF	−0.51	0.001
MPR	−0.55	<0.001
LGE	0.22	0.151
Infarct LGE	0.35	0.022
Atypical LGE	0.22	0.151
ECV	0.06	0.740

Multivariable Stepwise Regression	β	p Value	R^2
A. Including patient characteristics and angiographic data			
Time since transplantation	0.49	0.001	0.24
B. Including patient characteristics and CMR data			
Time since transplantation	0.47	<0.001	0.58
Early diastolic SR, 1/s	−0.24	0.049	
MPR	−0.57	<0.001	

Selected patient characteristics are shown. Additional data can be found in the Online Table 3. Separate multivariable analyses were performed for (A) angiographic and (B) CMR data.

SR = strain rate; other abbreviations as in Table 2.

characteristics including donor age, the presence of hypertension in the donor, and recipient:donor body mass index ratio showed significant associations with IMR on univariable analyses, as did CMR parameters such as EF, εcc, stress MBF, and MPR. On multivariable analysis only donor hypertension, EF, and MPR remained independently associated with IMR (Fig. 2B).

Diagnostic performance of cardiovascular magnetic resonance and angiography. In light of the multivariable regression results, MPR was the only CMR parameter used for ROC curve analysis. The diagnostic performance of angiography and CMR MPR are displayed in Table 5. When epicardial and microvascular disease were considered together, as in vivo, CMR MPR outperformed angiography (chi-square = 6.6, p = 0.01 for detecting moderate epicardial or microvascular disease; chi-square = 3.7, p = 0.05 for detecting severe epicardial or microvascular disease) (Fig. 3).

Associations with myocardial perfusion reserve. There was no association between MPR and maximum angiographic stenosis (β = −0.11, p = 0.469) or between MPR and FFR (β = 0.13, p = 0.415). On univariable analysis, donor age (β = −0.32, p = 0.038), LV mass index (β = −0.34, p = 0.021), εcc (β = −0.32, p = 0.049), infarct LGE (β = −0.29, p = 0.051), and ECV (β = −0.34, p = 0.045) were associated with MPR; but on multivariable stepwise regression only LV mass index (β = −0.39, p = 0.015) and infarct LGE (β = −0.36, p = 0.025) remained independently associated with MPR.

Table 4 Associations With Index of Microcirculatory Resistance

Univariable Associations	β	p Value
Patient characteristics		
Age	0.26	0.085
Time since transplantation	−0.18	0.224
Donor age	0.39	0.007
Donor hypertension	0.35	0.016
Recipient:donor BMI ratio	−0.31	0.043
Angiography		
Maximum angiographic stenosis	−0.16	0.281
CMR		
LVEF	−0.36	0.015
LVMI	0.16	0.288
εcc	0.46	0.002
Resting MBF	−0.05	0.762
Stress MBF	−0.54	<0.001
MPR	−0.55	<0.001
LGE	−0.12	0.463
Infarct LGE	−0.16	0.299
Atypical LGE	−0.12	0.463
ECV	0.10	0.588

Multivariable Stepwise Regression	β	p Value	R^2
Donor hypertension	0.29	0.012	0.58
EF	−0.26	0.024	
MPR	−0.60	<0.001	

Selected patient characteristics are shown. Additional data can be found in the Online Table 4. Abbreviations as in Table 2.

Discussion

This study provides comprehensive assessment of cardiac structure and function in the medium to long term after heart transplantation. The MPR, on the basis of measurement of absolute stress and rest MBF using CMR, was the only independent predictor of both epicardial and microvascular disease, and its diagnostic performance was significantly greater than that of invasive coronary angiography, the current clinical standard.

Invasive benchmarks. CAV is an exemplifier of a disease that affects both the epicardial and microvascular coronary

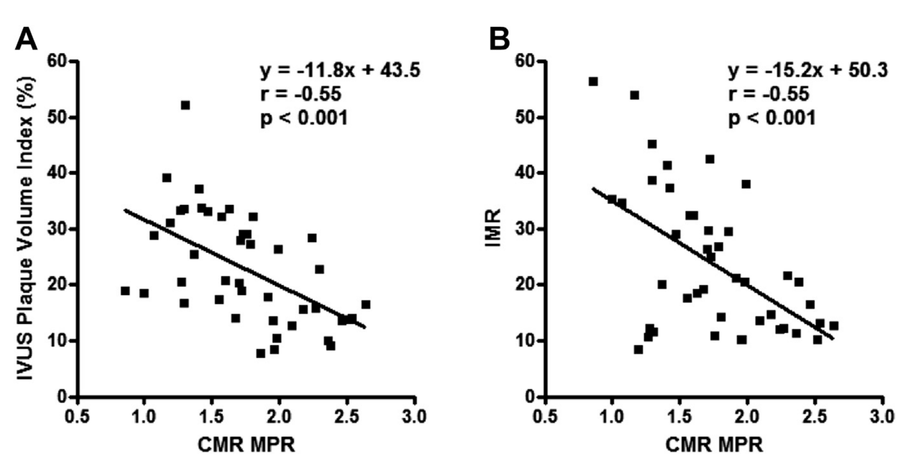

Figure 2 CMR MPR Plotted Against IVUS Plaque Volume Index and IMR

Cardiovascular magnetic resonance (CMR) myocardial perfusion reserve (MPR) plotted against **(A)** epicardial disease, assessed using intravascular ultrasound (IVUS) plaque volume index; and **(B)** microvascular disease, assessed using index of microcirculatory resistance (IMR).

Table 5 Diagnostic Performance of Coronary Angiography and Cardiovascular Magnetic Resonance Myocardial Perfusion Reserve

	AUC	Cut-Off	Sensitivity	Specificity
Diagnostic performance of angiographic stenosis for detecting				
Severe epicardial disease	0.70 (0.52–0.87)	21.09	0.69	0.63
Moderate epicardial disease	0.56 (0.39–0.72)	19.77	0.60	0.57
Severe microvascular disease	0.49 (0.30–0.67)	19.49	0.55	0.49
Moderate microvascular disease	0.44 (0.27–0.61)	19.40	0.57	0.48
Severe epicardial or microvascular disease	0.67 (0.52–0.82)	19.49	0.70	0.57
Moderate epicardial or microvascular disease	0.59 (0.42–0.77)	19.09	0.65	0.57
Diagnostic performance of CMR MPR for detecting				
Severe epicardial disease	0.79 (0.66–0.92)	1.58	0.77	0.78
Moderate epicardial disease	0.76 (0.60–0.91)	1.83	0.84	0.70
Severe microvascular disease	0.85 (0.70–0.99)	1.45	0.80	0.85
Moderate microvascular disease	0.71 (0.55–0.87)	1.74	0.71	0.64
Severe epicardial or microvascular disease	0.88 (0.78–0.98)	1.65	0.79	0.85
Moderate epicardial or microvascular disease	0.89 (0.79–1.0)	1.94	0.88	0.85

Receiver-operating characteristic curve analysis. Severe epicardial disease refers to >75th centile for intravascular ultrasound plaque volume index; moderate refers to above the median value. Severe microvascular disease refers to >75th centile for index of microcirculatory resistance; moderate refers to above the median value. Cut-off values for cardiovascular magnetic resonance (CMR) myocardial perfusion reserve (MPR) refer to MPR values less than or equal to this value. Cut-off values for maximum angiographic stenosis (%) refer to stenotic values greater than or equal to this value.
AUC = area under the curve.

compartments. In keeping with histological work and other invasive coronary physiology studies, the current study serves to confirm that CAV affects the epicardial arteries and the microvasculature independently (2,3,18,19). Comprehensive assessment of CAV, both in terms of evaluating disease severity and evaluating the performance of new diagnostic approaches, therefore requires assessment of both compartments. The current study is the first to evaluate a diagnostic approach to CAV with epicardial and microvascular benchmarks.

In the present study IVUS, rather than FFR, was used as the epicardial reference standard. IVUS is generally regarded as the gold standard technique for epicardial artery assessment in CAV and is considerably more established, and a number of studies have demonstrated that IVUS-derived vessel wall parameters, irrespective of hemodynamic significance, predict outcome in transplant recipients (20–24). In addition, because of the complex interplay between epicardial and microvascular disease, FFR may not provide a good indication of epicardial disease in CAV. Hirohata

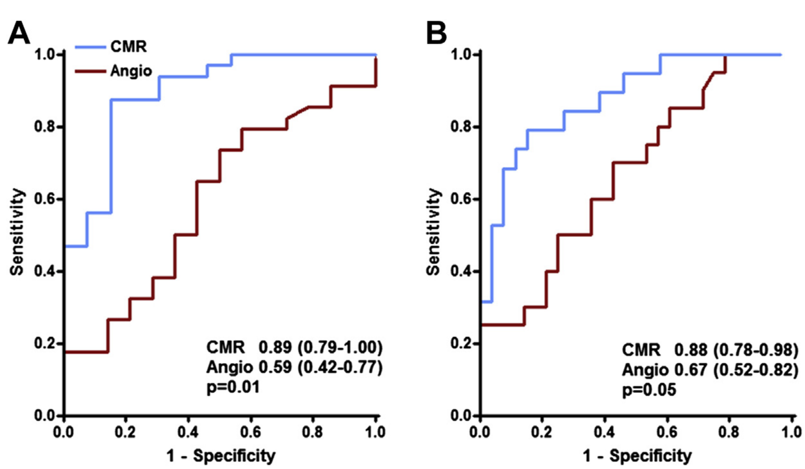

Figure 3 Diagnostic Performance of CMR MPR and Angiography for Detecting CAV

Diagnostic performance of cardiovascular magnetic resonance (CMR) **(blue lines)** myocardial perfusion reserve (MPR) and angiography (Angio) **(red lines)** for detecting **(A)** moderate cardiac allograft vasculopathy, defined as more than median epicardial or microvascular disease; and **(B)** severe cardiac allograft vasculopathy, defined as >75th centile epicardial or microvascular disease.

et al. (25) found that in patients >2 years post-transplant, for a given plaque burden, FFR varied significantly according to IMR; with FFR seen to improve (i.e., increase/become closer to 1.0) as IMR deteriorated (increased). These findings are directly in keeping with the findings of the current study, where FFR and IMR were shown to have a significant positive correlation. These observations reflect that in the setting of microvascular dysfunction, maximal achievable coronary flow is diminished, and thus the impact of an epicardial stenosis is lessened.

Such observations are not unique to CAV. For example, in the case of a given epicardial stenosis, FFR will be lower when the artery subtends viable myocardium (i.e., with minimal microvascular resistance, hence a large "pressure drop" down the artery) compared with if the artery were to supply infarcted myocardium (i.e., substantial microvascular resistance, hence a smaller pressure drop). Nevertheless, given the prevalence and importance of microvascular disease in CAV, these findings led Hirohata et al. (25) to conclude that "FFR may not provide a good representation of epicardial plaque burden late (i.e., more than 2 years) after heart transplantation." Indeed, over a number of studies, the correlation between FFR and IVUS parameters has varied considerably, from no correlation to a correlation coefficient of −0.58 (19,23).

In keeping with most other contemporary CAV studies, plaque volume index, rather than other IVUS parameters such as intima-media thickness, was used as it better reflects disease burden (12,19). In the absence of established disease severity cut-offs, 75th centile and median values were pragmatically chosen for ROC curve analysis. The IMR was used instead of invasive coronary flow reserve to assess the microvasculature because, unlike coronary flow reserve, IMR is specific for the microcirculation (i.e., independent of epicardial artery function) and largely independent of hemodynamic variations, and is more reproducible (10,26,27). Median and 75th centile IMR values were used for ROC curve analysis in keeping with other studies (28,29). Epicardial and microvascular disease severity in the current study was almost identical to that in the previous largest studies, and hence the disease severity thresholds used here appear reasonable (4,12,19,25).

Myocardial blood flow. The myocardial perfusion findings with regard to epicardial artery disease in the current study are in keeping with the results of 2 smaller studies that assessed MBF in CAV using ^{13}N-ammonia positron emission tomography. Kofoed et al. (30) and Wu et al. (31) found MPR and hyperemic MBF to be inversely related to IVUS parameters of CAV severity, with very similar univariable correlations to those found here (MPR: correlation coefficients up to −0.61 and −0.40, respectively, in the studies by Kofoed et al. and Wu et al. compared to a β value of −0.55 in the current study; hyperemic MBF: −0.49 and −0.46, respectively, compared to −0.51 in the current study). Also in keeping with the current study, in both positron emission tomography studies, resting MBF was higher in transplant patients than in control subjects, at least in part secondary to the higher resting heart rate seen in transplant recipients due to allograft vagal denervation, and was unrelated to the severity of epicardial artery disease.

A number of studies in other cardiovascular diseases have considered microvascular dysfunction to be present when MPR, or hyperemic MBF, are reduced in the presence of normal epicardial arteries (usually assessed with angiography) (32,33). Other studies have demonstrated a correlation between MPR and invasive coronary flow reserve (measured using intracoronary Doppler) in patients without significant epicardial coronary stenoses (34,35). To our knowledge, the current study is the first in any cardiac pathology to demonstrate that MPR, and hyperemic MBF, are independent predictors of microvascular function, when microvascular function itself is independently measured. Highlighting the importance of microvascular disease in CAV, MPR was governed by epicardial and microvascular disease to a similar degree.

The inverse association between MPR and LV mass index seen here has been described in other conditions where microvascular dysfunction is prominent (36–38), but this is the first time it has been demonstrated in transplanted hearts. There was also an association between the presence of infarct-typical LGE and reduced MPR; however, although myocardial extracellular volume was inversely associated with MPR on univariable analysis, the relationship did not remain significant on multivariable analysis. The discordance seen here between MPR and FFR is in keeping with that reported in other conditions and, as described by Johnson et al. (39), is likely to reflect the nature of the coronary pathophysiology involved.

Myocardial tissue characterization. Infarct prevalence in the current study (9%) was in keeping with the study by Butler et al. (11%) (40), although lower than in the study by Steen et al. (37%) (41); however, the cohort studied by Steen et al. represented advanced epicardial disease (including 19% with focal angiographic stenoses of ≥75%). The prevalence of infarct-atypical LGE in the current study (49%) was very similar to that found by Butler et al. (40%) (40) and by Steen et al. (51%) (41), and as in these other studies, was unrelated to epicardial disease. In addition to these other studies, which did not have a microvascular reference, the current study showed that infarct-atypical LGE was unrelated to microvascular disease.

Myocardial mechanics. In keeping with the findings of Weis et al. (42), who used CFR to assess microvascular dysfunction in patients with angiographically normal epicardial arteries, microvascular function was independently associated with LV function, which may reflect chronic subendocardial ischemia leading to impaired LV function. Early diastolic strain rate was independently associated with epicardial disease, which is in keeping with the study by Korosoglou et al. (43), but in general, myocardial deformation parameters were not discriminatory for CAV.

Why screen at all? It has been suggested that routine CAV screening should not be performed at all given the lack of evidence-based treatment options for improving symptoms or prognosis in established disease, other than retransplantation, which is possible in only a minority (44). Certainly significant luminal narrowing on angiography represents advanced vascular disease that is unlikely to be modifiable, and adverse events frequently occur well before this degree of disease is reached (9). This study demonstrates that CAV can potentially be detected noninvasively at a much earlier stage using CMR-based MBF assessment, which may allow earlier intensification of preventative therapy and may help pave the way for the development of disease-modifying therapies. However, although the CMR perfusion sequence used in the current study is in routine clinical use, and thus could be readily applied, CMR MBF quantification is technically challenging, and although considerable effort is being put into developing commercially available quantification software, at present it remains a research tool. Furthermore, it should be noted that 30% of patients screened had contraindications to CMR scanning or gadolinium contrast agent, and, therefore, such an approach would not be appropriate for all patients.

Study limitations. In keeping with the majority of studies involving transplant recipients, the current study is a relatively small, single–center study. The results require confirmation in larger, multicenter studies. The IVUS and invasive physiological assessments were performed on the LAD only; however, that also is in keeping with most other transplant studies (12). The IMR measurements were made without taking collateral flow into account (requiring balloon occlusion of the vessel); however, that is in keeping with all other studies using IMR in transplant recipients as collateralization is not a feature of CAV (12,19). Finally, this is a cross-sectional study and, therefore, the effect of disease progression on CMR MPR, and the prognostic value of CMR MPR, have not been assessed.

Conclusions

In this comprehensive assessment of cardiac structure and function in the medium to long term after transplantation, CMR-based MPR was independently predictive of both epicardial and microvascular components of CAV. Furthermore, the diagnostic performance of CMR MPR was significantly higher than that of coronary angiography, the current clinical screening technique.

Acknowledgments
The authors thank New Start Transplant Charity, the radiographers and administrative staff of the Alliance Wythenshawe CMR Unit, the secretarial and nursing staff of the Transplant Unit, and the Cardiology Waiting List coordinators in the North West Heart Centre. Finally, this study would not have been possible without the willing cooperation of the patients of the Transplant Unit, Wythenshawe, United Kingdom.

Reprint requests and correspondence: Dr. Christopher Miller, North West Heart Centre and The Transplant Centre, University Hospital of South Manchester, Wythenshawe, Manchester, Manchester M23 9LT, United Kingdom. E-mail: chrismiller@doctors.org.uk.

REFERENCES

1. Stehlik J, Edwards LB, Kucheryavaya AY, et al. The registry of the International Society for Heart and Lung Transplantation: 29th official adult heart transplant report—2012. J Heart Lung Transplant 2012;31:1052–64.
2. Hiemann NE, Wellnhofer E, Knosalla C, et al. Prognostic impact of microvasculopathy on survival after heart transplantation: evidence from 9713 endomyocardial biopsies. Circulation 2007;116:1274–82.
3. Abu-Qaoud MS, Stoletniy LN, Chen D, Kerstetter J, Kuhn M, Pai RG. Lack of relationship between microvascular and macrovascular disease in heart transplant recipients. Transplantation 2012;94:965–70.
4. Haddad F, Khazanie P, Deuse T, et al. Clinical and functional correlates of early microvascular dysfunction after heart transplantation. Circ Heart Fail 2012;5:759–68.
5. Tuzcu EM, De Franco AC, Hobbs R, et al. Prevalence and distribution of transplant coronary artery disease: insights from intravascular ultrasound imaging. J Heart Lung Transplant 1995;14 Suppl:202–7.
6. St. Goar FG, Pinto FJ, Alderman EL, et al. Intracoronary ultrasound in cardiac transplant recipients. In vivo evidence of "angiographically silent" intimal thickening. Circulation 1992;85:979–87.
7. Costanzo MR, Dipchand A, Starling R, et al. The International Society of Heart and Lung Transplantation Guidelines for the care of heart transplant recipients. J Heart Lung Transplant 2010;29:914–56.
8. Miller CA, Chowdhary S, Ray SG, et al. Role of noninvasive imaging in the diagnosis of cardiac allograft vasculopathy. Circ Cardiovasc Imaging 2011;4:583–93.
9. Tuzcu EM, Kapadia SR, Sachar R, et al. Intravascular ultrasound evidence of angiographically silent progression in coronary atherosclerosis predicts long-term morbidity and mortality after cardiac transplantation. J Am Coll Cardiol 2005;45:1538–42.
10. Fearon WF. Novel index for invasively assessing the coronary microcirculation. Circulation 2003;107:3129–32.
11. Messroghli DR, Greiser A, Frohlich M, Dietz R, Schulz-Menger J. Optimization and validation of a fully-integrated pulse sequence for modified look-locker inversion-recovery (MOLLI) T1 mapping of the heart. J Magn Reson Imaging 2007;26:1081–6.
12. Fearon WF. Simultaneous assessment of fractional and coronary flow reserves in cardiac transplant recipients: Physiologic Investigation for Transplant Arteriopathy (PITA study). Circulation 2003;108:1605–10.
13. Miller CA, Jordan P, Borg A, et al. Quantification of left ventricular indices from SSFP cine imaging: impact of real-world variability in analysis methodology and utility of geometric modeling. J Magn Reson Imaging 2013;37:1213–22.
14. Miller CA, Borg A, Clark D, et al. Comparison of local sine wave modeling with harmonic phase analysis for the assessment of myocardial strain. J Magn Reson Imaging 2013;38:320–8.
15. Biglands J, Magee D, Boyle R, Larghat A, Plein S, Radjenovic A. Evaluation of the effect of myocardial segmentation errors on myocardial blood flow estimates from DCE-MRI. Phys Med Biol 2011;56:2423–43.
16. Jerosch-Herold M, Swingen C, Seethamraju RT. Myocardial blood flow quantification with MRI by model-independent deconvolution. Med Phys 2002;29:886–97.
17. Wong TC, Piehler K, Meier CG, et al. Association between extracellular matrix expansion quantified by cardiovascular magnetic resonance and short-term mortality. Circulation 2012;126:1206–16.
18. Kubrich M, Petrakopoulou P, Kofler S, et al. Impact of coronary endothelial dysfunction on adverse long-term outcome after heart transplantation. Transplantation 2008;85:1580–7.

19. Fearon WF, Hirohata A, Nakamura M, et al. Discordant changes in epicardial and microvascular coronary physiology after cardiac transplantation: Physiologic Investigation for Transplant Arteriopathy II (PITA II) study. J Heart Lung Transplant 2006;25:765–71.
20. Rickenbacher PR, Pinto FJ, Lewis NP, et al. Prognostic importance of intimal thickness as measured by intracoronary ultrasound after cardiac transplantation. Circulation 1995;92:3445–52.
21. Mehra MR, Ventura HO, Stapleton DD, Smart FW, Collins TC, Ramee SR. Presence of severe intimal thickening by intravascular ultrasonography predicts cardiac events in cardiac allograft vasculopathy. J Heart Lung Transplant 1995;14:632–9.
22. Kobashigawa JA, Tobis JM, Starling RC, et al. Multicenter intravascular ultrasound validation study among heart transplant recipients. J Am Coll Cardiol 2005;45:1532–7.
23. Lee C-M, Wu Y-W, Jui H-Y, et al. Intravascular ultrasound correlates with coronary flow reserve and predicts the survival in angiographically normal cardiac transplant recipients. Cardiology 2008;109:93–8.
24. Sarno G, Lerman A, Bae JH, et al. Multicenter assessment of coronary allograft vasculopathy by intravascular ultrasound-derived analysis of plaque composition. Nat Clin Pract Cardiovasc Med 2009;6:61–9.
25. Hirohata A, Nakamura M, Waseda K, et al. Changes in coronary anatomy and physiology after heart transplantation. Am J Cardiol 2007;99:1603–7.
26. Aarnoudse W. Epicardial stenosis severity does not affect minimal microcirculatory resistance. Circulation 2004;110:2137–42.
27. Ng MKC. Invasive assessment of the coronary microcirculation: superior reproducibility and less hemodynamic dependence of index of microcirculatory resistance compared with coronary flow reserve. Circulation 2006;113:2054–61.
28. Fearon WF, Shah M, Ng M, et al. Predictive value of the index of microcirculatory resistance in patients with ST-segment elevation myocardial infarction. J Am Coll Cardiol 2008;51:560–5.
29. McGeoch R, Watkins S, Berry C, et al. The index of microcirculatory resistance measured acutely predicts the extent and severity of myocardial infarction in patients with ST-segment elevation myocardial infarction. J Am Coll Cardiol Intv 2010;3:715–22.
30. Kofoed KF, Czernin J, Johnson J, et al. Effects of cardiac allograft vasculopathy on myocardial blood flow, vasodilatory capacity, and coronary vasomotion. Circulation 1997;95:600–6.
31. Wu YW, Chen YH, Wang SS, et al. PET assessment of myocardial perfusion reserve inversely correlates with intravascular ultrasound findings in angiographically normal cardiac transplant recipients. J Nucl Med 2010;51:906–12.
32. Panting JR, Gatehouse PD, Yang GZ, et al. Abnormal subendocardial perfusion in cardiac syndrome X detected by cardiovascular magnetic resonance imaging. N Engl J Med 2002;346:1948–53.
33. Cecchi F, Olivotto I, Gistri R, Lorenzoni R, Chiriatti G, Camici PG. Coronary microvascular dysfunction and prognosis in hypertrophic cardiomyopathy. N Engl J Med 2003;349:1027–35.
34. Shelton ME, Senneff MJ, Ludbrook PA, Sobel BE, Bergmann SR. Concordance of nutritive myocardial perfusion reserve and flow velocity reserve in conductance vessels in patients with chest pain with angiographically normal coronary arteries. J Nucl Med 1993;34:717–22.
35. Jerosch-Herold M, Wilke N, Stillman AE. Magnetic resonance quantification of the myocardial perfusion reserve with a Fermi function model for constrained deconvolution. Med Phys 1998;25:73–84.
36. Knaapen P, Germans T, Camici PG, et al. Determinants of coronary microvascular dysfunction in symptomatic hypertrophic cardiomyopathy. Am J Physiol Heart Circ Physiol 2008;294:H986–93.
37. Nakajima H, Onishi K, Kurita T, et al. Hypertension impairs myocardial blood perfusion reserve in subjects without regional myocardial ischemia. Hypertens Res 2010;33:1144–9.
38. Steadman CD, Jerosch-Herold M, Grundy B, et al. Determinants and functional significance of myocardial perfusion reserve in severe aortic stenosis. J Am Coll Cardiol Img 2012;5:182–9.
39. Johnson NP, Kirkeeide RL, Gould KL. Is discordance of coronary flow reserve and fractional flow reserve due to methodology or clinically relevant coronary pathophysiology? J Am Coll Cardiol Img 2012;5:193–202.
40. Butler CR, Kumar A, Toma M, et al. Late gadolinium enhancement in cardiac transplant patients is associated with adverse ventricular functional parameters and clinical outcomes. Can J Cardiol 2013;29:1076–83.
41. Steen H, Merten C, Refle S, et al. Prevalence of different gadolinium enhancement patterns in patients after heart transplantation. J Am Coll Cardiol 2008;52:1160–7.
42. Weis M, Hartmann A, Olbrich HG, Hor G, Zeiher AM. Prognostic significance of coronary flow reserve on left ventricular ejection fraction in cardiac transplant recipients. Transplantation 1998;65:103–8.
43. Korosoglou G, Osman NF, Dengler TJ, et al. Strain-encoded cardiac magnetic resonance for the evaluation of chronic allograft vasculopathy in transplant recipients. Am J Transplant 2009;9:2587–96.
44. Grant SC, Brooks NH, Levy RD. Routine coronary angiography after heart transplantation. Heart 1997;78:101–2.

Key Words: cardiac allograft vasculopathy ▪ cardiovascular magnetic resonance ▪ diagnosis ▪ microvascular disease ▪ myocardial blood flow.

APPENDIX

For supplemental tables, please see the online version of this article.